HHS Public Access

Author manuscript

Nat Neurosci. Author manuscript; available in PMC 2010 March 01.

Published in final edited form as:

Nat Neurosci. 2009 September ; 12(9): 1159–1164. doi:10.1038/nn.2353.

High sensitivity rod photoreceptor input to the blue-yellow color opponent pathway in macaque retina

Greg D. Field[1], **Martin Greschner**[1], **Jeffrey L. Gauthier**[1], **Carolina Rangel**[2], **Jonathon Shlens**[1,3], **Alexander Sher**[4], **David W. Marshak**[2], **Alan M. Litke**[4], and **E.J. Chichilnisky**[1]

[1] Salk Institute for Biological Studies, La Jolla, CA

[2] Department of Neurobiology and Anatomy, University of Texas Medical School, Houston, TX

[3] University of California, Berkeley, CA

[4] Santa Cruz Institute for Particle Physics, University of California, Santa Cruz, CA

Abstract

Small bistratified cells (SBCs) in the primate retina carry a major blue-yellow opponent signal to the brain. Here we show that SBCs also carry signals from rod photoreceptors, with the same sign as S cone input. SBCs exhibited robust responses under low scotopic conditions (<0.01 P*/rod/s). Physiological and anatomical experiments indicated that this rod input arose from the AII amacrine cell mediated rod pathway. Rod and cone signals were both present in SBCs at mesopic light levels. We discuss three implications of these findings. First, more retinal circuits than previously thought may multiplex rod and cone signals, efficiently exploiting the limited number of optic nerve fibers. Second, signals from AII amacrine cells may diverge to most or all of the <20 RGC types in the peripheral primate retina. Third, rod input to SBCs may be the substrate for behavioral biases toward perception of blue at mesopic light levels.

Introduction

The mammalian retina contains <20 morphologically distinct retinal ganglion cell (RGC) types1–3. Each RGC type receives input from a distinct set of retinal interneuron types, encodes a different aspect of the visual scene, and projects to a distinct set of targets in the brain. Among the RGC types in the primate retina, small bistratified cells (SBCs) are of particular interest: they display cone opponent responses appropriate for blue-yellow color vision4; they are the fifth most numerous RGC type in the primate2; and they form a major projection to the koniocellular layers of the lateral geniculate nucleus (LGN)5.

Contact: G.D. Field, Systems Neurobiology, The Salk Institute, 10010 North Torrey Pines Road, La Jolla, CA 92037, USA. gfield@salk.edu, phone: (858) 453-4100 x1074.

Author Contributions: G.D.F, D.M.W, and E.J.C. conceived the experiments and wrote the manuscript. G.D.F., M.G., J.L.G, J.S, A.S, and E.J.C. performed the electrophysiological experiments. C.R. and D.W.M. performed the immunolabeling experiments. A.S. and A.L.M. provided and supported the large-scale multielectrode array system.

A fundamental aspect of SBC function is unknown: whether in addition to their role in photopic (cone mediated) vision, SBCs contribute to scotopic (rod mediated) vision. The possibility that SBCs carry rod signals is suggested by psychophysical studies demonstrating perceptual shifts toward blue hues in mesopic (rod and cone mediated) vision6. However, previous measurements from blue-yellow color opponent cells in the primate retina revealed little or no input from rods7, while recordings from possible SBC target neurons in the LGN have produced mixed results8,9.

Rod input to SBCs has potentially important implications for the function and organization of parallel pathways in the primate visual system. If SBCs avoid rod input, it would indicate that a substantial fraction (<10%)2 of the axons in the optic nerve carry no behaviorally relevant signal during night vision. It would also indicate that one function of the parallel pathway organization is to specialize certain RGC types for a limited range of light levels. Furthermore it would suggest avoidance of two kinds of rod inputs in the presynaptic circuity of SBCs: gap junctions between rods and S cones, and gap junctions between AII amacrine cells and S cone bipolar cells. Conversely, if SBCs do receive rod input, this input may help to explain perceptual biases toward blue hues under mesopic conditions, and would suggest that the visual system multiplexes signals in each cell type to use the optic nerve efficiently.

We used large-scale multielectrode recordings10 from peripheral primate retina to test whether SBCs receive rod input. This approach allowed for long, stable recordings from identified SBCs, an important technical advantage. We recorded from nearly complete populations of SBCs with receptive fields that collectively covered the recorded region of retina11. All SBCs received rod input with the same ON type response polarity as S cone input. SBC receptive field sizes were significantly larger at rod dominated light levels, revealing a change in spatial processing in night vs. day vision. Furthermore, physiological and anatomical experiments indicated that rod signals reach SBCs via a known high-sensitivity pathway: rod signals are conveyed by rod-specific bipolar cells to AII amacrine cells, which in turn form gap junctions with ON cone bipolar cells that provide excitatory input to RGCs12,13. We discuss the implications of these findings for retinal circuitry, night vision, and color perception.

Results

To test for rod input to SBCs, recordings were made from RGCs in peripheral primate retina with a 512-electrode array at two light levels (Fig. 1): a “high” light level at which signaling was dominated by cone photoreceptors (photopic; <1000 P*/cone/s), and a “low” light level at which signaling was dominated by rod photoreceptors (scotopic; <1.0 P*/rod/s). Receptive fields were estimated by computing the spike triggered average (STA) of a white noise stimulus presented at both the high and low light levels (see Methods).

SBCs were identified at the high light level by observing a functional class of RGCs with blue-ON/yellow-OFF receptive fields that formed a mosaic uniformly covering the retina (Fig. 1b, black circles), and with a density corresponding to that of the small bistratified morphological type11. Blue-ON/yellow-OFF responses were identified by increments in the

blue display primary and decrements in the red and green primaries preceding spikes (Fig. 1c–**e**, bottom left panels). Such responses are consistent with an ON response mediated by S cones and an OFF response mediated by L and M cones11,14.

Successful tracking of SBCs between the high and low light levels was confirmed by two independent observations. First, a functional classification of RGCs recorded at the low light level (Fig. 1g) produced a class with a nearly identical spatial organization of receptive fields (Fig. 1a,**f**). Second, neurons at the low light level with corresponding receptive field locations exhibited nearly identical electrophysiological images (EIs: Fig. 1c–**e**,**h**–**j**, top panels). The EI is the spike triggered average spatiotemporal pattern of electrical activity elicited by an identified cell, which provides a unique electrical "footprint" for each RGC10 (see Methods). These two independent lines of evidence indicate that SBCs identified at the high light level were correctly associated with cells identified at the low light level.

SBCs receive rod input

The high light level produced a photon flux corresponding to <100 Trolands (photopic)15. In addition, the blue-ON/yellow-OFF opponent response displayed by the SBCs could not be mediated solely by the rods (Fig. 1c–**e**).

The low light level produced a photon flux that corresponded to <0.1 scotopic Trolands, well below the psychophysically determined cone threshold of <10 scotopic Trolands16. At the low light level, the time course of the SBC light response was more monophasic and the time to peak was 4.1 ± 0.6 (mean ± s.d.) fold longer than at the high light level, suggesting a switch from cone to rod dominated signaling7,17,18. Furthermore, the STAs of the SBCs at the low light level did not display a color opponent response (Fig. 1h–**j**, bottom left panels). Instead, they exhibited a relative sensitivity to the red, green, and blue display primaries [0.074 ±0.05, 1.0, 0.83 ±0.04 (s.e.m.); normalized by the green primary] consistent with that predicted from the spectral sensitivity of rods (0.070, 1.0, 0.84). Simultaneously recorded ON and OFF parasol cells exhibited nearly identical relative sensitivities to the display primaries at the low light level (ON parasol: 0.073 ±0.005, 1.0, 0.82 ±0.004; OFF parasol: 0.10 ±0.01, 1.0, 0.84 ±0.01), further supporting the interpretation that rod signals provided the dominant or exclusive input.

SBC receptive fields are larger under scotopic conditions

SBC receptive fields were larger under scotopic compared to photopic conditions (Fig. 2), consistent with previous observations in other RGC types18–20. The blue-ON (S cone mediated) receptive fields (light gray) are superimposed on the rod mediated receptive fields (dark gray) to facilitate comparison (Fig. 2a). Note that the white noise stimulus used in these experiments did not reveal a receptive field surround in SBCs under scotopic conditions, consistent with observations from other RGC types19,21 (but see20). For most cells, the cone mediated receptive field was smaller than the rod mediated receptive field and this trend was observed across all 8 analyzed preparations (Fig. 2b,**c**). On average, the rod mediated receptive fields were <20% larger in radius than cone mediated receptive fields. The dependence of receptive field size on light level was reversible in two preparations tested (32 SBCs) in which the attachment between pigment epithelium and

retina was preserved (Fig. 2d; see Methods). Thus, SBCs exhibited a significant and reversible change in receptive field size between rod and cone mediated responses.

Rod responses persist in SBCs in low scotopic conditions

The presence of robust rod-driven responses at light levels <1.0 P*/rod/s suggested that the high sensitivity rod pathway mediated by AII amacrine cells may contribute signals to the presynaptic circuitry of SBCs13,16,22. This pathway is thought to dominate visual signaling under scotopic conditions. However, recent recordings from primate cones23 and mouse RGCs24 suggest that gap junctions between rods and cones could also provide reliable rod signals at <1.0 P*/rod/s.

White noise stimulation at <0.1 P*/rod/s elicited clear light responses in SBCs (Fig 2a, Retina 4). This light level is significantly below the threshold of the rod-to-cone gap junction pathway23,24. The fact that light responses and mosaics of SBC receptive fields were recorded at this light level supports the hypothesis that the AII amacrine cell pathway provides rod input to SBCs. A second recording from 10 SBCs produced similar results (Fig. 2c).

We also tested whether SBCs responded reliably to a stimulus consisting of light steps about a mean light level of 0.01 P*/rod/s. SBCs produced robust responses to these light steps (Fig 3a). Furthermore these responses were similar to those produced by simultaneously recorded ON parasol cells (Fig. 3b), which project to the magnocellular layers of the LGN and exhibit high contrast sensitivity under both photopic and scotopic conditions. Therefore, these results demonstrate that SBCs receive high sensitivity rod signals.

L-APB blocks light responses at light levels < 1 P*/rod/s

To further test whether AII amacrine cells mediate the observed rod input to SBCs, responses of OFF parasol cells to full field light steps were measured with and without bath application of 10 μM L-APB ((l-(+)-2-amino-4phosphonobutyric acid) (Fig. 4). L-APB is a group III metabotropic glutamate receptor agonist that saturates the postsynaptic receptors (mGluR6) of ON type bipolar cells, effectively blocking synaptic transmission between photoreceptors and all ON type (including rod) bipolar cells25. If rod signals at a particular light level are conveyed to RGCs exclusively by the rod bipolar –> AII amacrine cell circuit, then L-APB should block the light response of OFF type RGCs in addition to the typical effect of blocking light responses in ON type RGCs26. Alternatively, to the extent that rod signals are conveyed to cones via gap junctions, responses in OFF type RGCs should not be blocked by L-APB because rod signals will be conveyed to OFF type RGCs via synapses utilizing ionotropic glutamate receptors, which are insensitive to L-APB.

OFF parasol cells exhibited robust responses to light steps about a mean light level of 0.14 P*/rod/s (Fig. 4a). These responses were eliminated by L-APB (Fig. 4b). Note that light responses were undetectable even when averaging over 20 cycles of the step stimulus from 24 simultaneously recorded OFF parasol cells (Fig. 4b; black trace). Responses to light steps about a gray value 10 folder higher (1.4 P*/rod/s) were also reduced by L-APB (Fig 4c,**d**). However, at this higher light level averaging across trials and cells revealed a very weak

response modulation to the light steps (Fig. 4d; black trace). At both light levels, maintained background activity of the OFF parasol cells increased with application of L-APB26, and the light response recovered when L-APB was washed from the bath (data not shown). As expected the responses of SBCs and ON parasol cells were also eliminated by L-APB at both light levels (data not shown). In the presence of L-APB, the maintained spike rate increased for OFF parasol cells, and was zero for both SBCs and ON parasol cells (data not shown), consistent with previous studies26. These results indicate that light responses to stimuli generating fewer than a <1–2 P*/rod/s are mediated predominantly, if not exclusively, by the AII amacrine cell pathway, consistent with previous observations in mouse27. However, the L-APB-insensitive rod signals at higher light levels suggest a contribution of rod-cone gap junctions (see Discussion).

Gap junctions between AII amacrine and S cone bipolar

A prediction that emerges from the above results is the presence of gap junctions between AII amacrine cells and S cone bipolar cells. However, previous studies have suggested that AII amacrine cells may avoid forming gap junctions with S cone bipolar cells28. Therefore, we performed experiments to search for such contacts by labeling S cone bipolar cells, AII amacrine cells, and the connexin 36 protein, which forms the gap junction between AII amacrine cells and ON-cone bipolar cells24.

The glycine-extended gastrin-cholecystokinin precursor, G6-gly, was used to label S cone bipolar cells (Fig. 5, green)29. Antibodies to calretinin labeled AII amacrine cells (blue)30. Cell types were confirmed based ON morphological characteristics (see Supplemental Methods online). Antibodies to connexin 36 (red) were used to label putative gap junctions in the inner plexiform layer31.

In stratum 5 (S5) of the IPL there were appositions between S cone bipolar cell axons and dendrites of AII amacrine cells, and puncta containing immunoreactive connexin 36 were found at these sites (Fig. 5a). These contacts were followed through consecutive optical sections (0.5 μm steps) to avoid misinterpretation due to superposition of non-serial image planes (Fig. 5b–**e**). Similar contacts were observed in the retinas of all three animals used in these experiments (Supplemental Figs. 1–4). Therefore, AII amacrine cells appear to make gap junctions with S cone bipolar cells, endowing SBCs with high sensitivity rod signals.

Simultaneous rod and cone input to SBCs

The observed rod input to SBCs under low scotopic conditions suggests that rod and cone signals may mix at mesopic light levels. Alternatively, the mechanisms carrying rod signals to SBCs could saturate prior to reaching the threshold for cone activation, preventing mixing of rod and cone signals. We tested for simultaneous rod and cone input by measuring SBC receptive fields across a range of light levels (Fig. 6). At the highest light levels, SBCs displayed a relative sensitivity to the red, green and blue display primaries consistent with a SON/(L+M)-OFF cone mediated response11,14. However, between 150 and 300 P*/rod/s, SBCs exhibited a marked change in spectral tuning: increments, rather than decrements, in the green display primary tended to precede spikes.

In principle, this change in spectral tuning could be explained two ways: (1) a weakening of the L+M-OFF surround and/or (2) the inclusion of rod input with the same sign as S cone input. In the former case, the sensitivity to the green display primary should approach the value predicted from the spectral sensitivity of the S cones. The expected sensitivity to the green relative to blue display primary for S cones is 0.11 (see Methods). However, at 150 P*/rod/s the observed ratio was 0.35 ±0.04 (s.e.m.). Thus, the large sensitivity to increments of the green display primary implies rod input to the SBCs. Cones must also provide input to SBCs at 150 P*/rod/s because the response remains color opponent (OFF type response to modulation of the red display primary), and the spectral tuning of the response does not match that expected from rods (Fig. 6 STA time course at 1.5 P*/rod/s). At progressively lower mean light levels, the relative sensitivity to the three display primaries shifted to the values expected from pure rod input. Therefore, rod and cone signals mix in SBCs at light levels between <75 and <300 P*/rod/s.

Discussion

We have demonstrated that visual encoding in SBCs extends to low scotopic conditions, that SBC receptive fields are larger under these conditions, and that AII amacrine cells convey rod input to the presynaptic circuitry of SBCs. Below, these results are compared to those of previous studies and we elaborate on implications for scotopic visual processing, retinal circuitry and color perception.

The origin of rod input to SBCs

The AII amacrine cell rod pathway (rod –> rod bipolar –> AII amacrine –> cone bipolar –> RGC) mediates visual processing near absolute threshold and throughout low scotopic vision12,13. Several lines of evidence presented here indicate that this pathway contributes rod signals to SBCs, the major blue-ON/yellow-OFF pathway of the primate visual system.

SBCs produced vigorous responses to light steps (Fig. 3) and white noise stimulation (Fig. 2) at light levels at which L-APB blocked the response of OFF parasol cells (Fig. 4), suggesting that at these light levels the AII amacrine cell pathway is the dominant pathway for signals to reach RGCs. Furthermore, human psychophysical and electroretinogram studies suggest that the rod-cone gap junction pathway is not strongly activated at light levels < 1 scotopic Troland16, which corresponds to <10 P*/rod/s32. Finally, anatomical experiments indicated the presence of connexin-36 at appositions of AII amacrine cell dendrites and S cone bipolar cell axon terminals (Fig. 5 and Supplemental Figs. 1–4), thus providing anatomical evidence for the existence of this pathway.

However, these results do not rule out the possibility that gap junctions between rods and S cones contribute rod signals to SBCs at light levels > 1–2 P*/rod/s. Indeed, gap junctions between rods and S cones have been observed in anatomical studies of primate retina (S. Massey, personal communication). Also in primate, rod activation hyperpolarizes S cones, presumably through gap junctions (Verweij J, et al. ARVO 2008, #3250). The relative contribution of rod to cone gap junctions and the AII amacrine cell pathway at mesopic and high scotopic lighting conditions remains unclear.

Comparison to previous studies

Previous studies of rod input into blue-yellow opponent cells in the primate visual system produced mixed results. One study of the LGN identified some rod input9 while other studies of the LGN and the retina revealed little or no rod input7,8. There are several possible technical limitations of previous studies which could produce discrepant results: (1) insufficient time for dark-adaptation which could cause rod input to be underestimated; (2) the challenge of maintaining stable recordings for long periods of time *in vivo*, (3) recordings near the fovea where rods are sparse, and (4) recordings from unidentified morphological cell types, which could produce variable results if some blue-ON/yellow-OFF cell types receive rod input while others do not. These potential issues were mitigated in the present study. First, the retina was dark-adapted for > 40 minutes before recordings were made under scotopic conditions (see Methods). Second, the use of a large-scale multielectrode array provided recordings for 5–15 hours from collections of cells where stability could be confirmed by (1) stable EIs of individual cells and (2) the stable position of individual cell receptive fields within a mosaic of other receptive fields with matched response properties. Third, recordings were made from peripheral primate retina where the rod density is high and relatively uniform15. Fourth, the observation of nearly complete receptive field mosaics allowed the density of blue-yellow opponent cells to be determined, which provided an unambiguous association with a morphologically defined cell type, the SBC11.

The anatomical data presented here indicate that AII amacrine cells make gap junctions with S cone bipolar cells. This was not observed in two earlier electron microscopic studies of macaque S cone bipolar cells, probably for technical reasons. In one study, S cone bipolar cells in peripheral retina were filled with electron-dense peroxidase reaction product, which made detection of gap junctions difficult, and the sample was limited due to the low spatial density of the terminals29. In another study, three central S cone bipolar cell axon terminals were completely reconstructed from serial sections, but gap junctions were not described33. Central and peripheral retina may differ in this respect. An additional electron microscopic study of area centralis in cat retina identified a single ON cone bipolar cell type (b5) that was neither directly nor indirectly coupled to AII amacrine cells and that exhibited a morphology similar to the S cone bipolar cell28. However, conclusions regarding this cell type were generalized from a single b5 cell.

In the rabbit retina, the connexin-36 gap-junction permeant tracer Neurobiotin labeled putative S cone bipolar cells when injected into AII amacrine cells (S. Mills: ARVO 1994, #2625). Combined with the present findings, this suggests that rod input to the S cone pathway is a general feature of the mammalian visual system.

Night vision may utilize most visual pathways

Does the visual system utilize all the fibers of the optic nerve for scotopic vision or does it reserve some fibers for cone signals to reduce rod-cone signal mixing and deleterious consequences for color vision? Many studies have highlighted the challenges faced by the visual system at night: a sparse collection of absorbed photons must be detected on a background of substantial cellular and synaptic noise22. This combined with anatomical and

physiological observations that AII amacrine cells form synapses with many cone bipolar cell types28,34,35, suggests most or all RGC types may participate in scotopic vision. However, several physiological studies have suggested that only a fraction of RGC types may participate in low scotopic vision7,8,18,24.

In peripheral primate retina, it appears that rod signals diverge to many and perhaps all RGC types. Previous anatomical and physiological studies suggest rod input via the AII pathway to peripheral parasol cells7,36, midget cells37,38, giant sparse (melanopsin) cells39, and upsilon cells (Field, et al ARVO 2008 #3856). The results presented here reveal rod input to SBCs. Furthermore, rod signals are provided to SBCs by gap junctions between AII amacrine cells and Scone bipolar cells. Therefore, large bistratified cells (LBCs) in the primate retina should also receive rod input from the AII amacrine pathway, because S cone bipolar cells are thought to provide presynaptic input to both SBCs and LBCs40,41. In sum, rod input via the AII pathway has been observed for each RGC type in the peripheral primate retina that has been studied under scotopic conditions.

It remains unclear whether these results will generalize to the central primate retina7, and whether there are major differences in the promiscuity of AII amacrine cell signals to various RGC types in primate versus other mammals. Perhaps surprisingly, SBCs exhibited a sensitivity under low scotopic conditions qualitatively similar to that of ON parasol cells (Fig. 3). However, the present results do not quantitatively compare the signal to noise properties of SBCs to those of ON parasol cells or other RGC types a comparison that will determine which RGC types provide the most reliable signals to the brain when photons are scarce.

Rod input to SBCs may explain blue bias in night vision

Observations that scenes appear bluish at mesopic light levels date to the nineteenth century42. Furthermore, psychophysical experiments show that rod activation biases color judgments toward blue hues6, and influences color discriminations involving changes in S cone activation43,44. Models explaining these results postulate rod input to SBCs45,46, however as described above, previous physiological experiments have largely failed to observe such input. The light levels at which the effects of rod activation on S cone signals and blue hue biases are maximized are 2–10 Trolands46, corresponding to <60–300 P*/rod/s, the light levels for which the opponent spectral tuning of SBCs was most influenced by rod activation (Fig. 6). Thus, the present work may help explain the psychophysical results. Activation of the rods, like activation of S cones, results in an increased spike rate in SBCs. Thus, to the degree that SBC spikes contribute to the perception of blue, rod activation would be expected to produce a bias toward the perception of blue.

Methods

Physiology

Retinas were obtained and recorded as described previously11. Briefly, eyes were enucleated from terminally anesthetized macaque monkeys (*Macaca mulatta* and *Macaca*

fascicularis) used in the course of other experiments11, in accordance with institutional guidelines for the care and use of animals. Immediately after enucleation, the anterior portion of the eye and vitreous were removed in room light. Following a dark-adaptation period > 40 minutes at 32–33 C, segments of peripheral retina that were well attached to the pigment epithelium were isolated and placed flat, RGC layer down, on a planar array of 512 extracellular microelectrodes covering a region 1890 μm x 900 μm. While recording, isolated retina was kept at 33–35 C and was perfused with Ames' solution bubbled with 95% O and 5% CO, pH 7.4. 10 μM L-APB was added to the Ames' solution for some experiments (Fig. 4b–**d**). The L-APB solution was washed in (out) of the recording chamber for < 5 mins before data collection resumed. In experiments designed to test the reversibility of receptive field size and SBC response properties at mesopic conditions (Figs. 2d and 6), the retina was left attached to the pigment epithelium and choroid and recorded at temperatures 31–35C.

Recordings were analyzed offline to isolate the spikes of different cells, as described previously11. Briefly, candidate spike events were detected using a threshold on each electrode, and the voltage waveform on the center and nearby electrodes in the vicinity of spike events was extracted. Spikes were clustered based on waveform shape, and spike clusters were identified as candidate neurons if they exhibited a refractory period and an average spike rate >0.25 Hz. Duplicate recordings of the same cell were identified by temporal cross-correlation and removed.

Light calibration and stimuli

An optically reduced stimulus from a gamma-corrected cathode ray tube computer display (Sony Multiscan E100) refreshing at 120 Hz was focused on the photoreceptor outer segments. Light intensity was controlled by neutral density filters in the light path. The emission spectrum of each display primary was measured with a PR-701 spectra-radiometer (PhotoResearch, Chatsworth, CA) after passing through the optical elements between the display and the retina. The power of each display primary was measured at the preparation with a calibrated photodiode (UDT Instruments, San Diego, CA). For rods, the photoisomerization rate (P*/rod/s) was estimated by computing the inner product of the power scaled emission spectra per unit area with the spectral sensitivity of macaque rhodopsin47 and multiplying by the effective collecting area of the primate rod (1.2 μm)47.

The mean photoisomerization rate for the L, M and S cones at the photopic light levels (i.e. Fig. 1) was calculated in the same manner described for the rods, with an estimated effective cone collecting area of 0.37 μm48,49. These calculations yielded bleaching rates for the L, M and S cones of 800, 800, and 440 P*/cone/s, respectively at the photopic condition.

In experiments with the pigment epithelium attached to the retina, the visual stimulus passed through the mostly transparent electrode array and the retina before being absorbed in the photoreceptor outer segments. The emission spectra of the display primaries and their emission powers were calibrated as described above, but for a different optical path. At the highest mean light level presented, the bleaching rates for the L, M, and S cones and the rods were 1400, 1200, 400 P*/cone/s, and 3000 P*/rod/s, respectively (Fig. 6). In these experiments, the predicted relative sensitivities to the red, green, and blue display primaries

for the rods was 0.070, 1.0 and 0.84 (normalized to the green primary), respectively. For the L, M and S cones, the predicted relative sensitivities were (0.41, 1.0, 0.18), (0.15, 1.0, 0.29), and (0.02, 0.11, 1.0; normalized to the blue primary).

These estimates of the rod and cone photoisomerization rates did not correct for the angle of illumination and pigment self screening in the photoreceptor outer segments, because the precise angle of illumination and the amount of bleached pigment were unknown. In addition, estimates of pigment density of the rods and cones vary by roughly a factor of 2. However, assuming axial rather than transverse illumination and a pigment density of 0.1748 (0.3747) for the cones (rods), changed the photoisomerization rates by < 50%.

In some experiments (Figs. 3 and 4) light steps were presented as stimuli. These step stimuli were full field and periodic, transitioning from one light level to another either every 3 s (Fig. 4) or 5 s (Fig. 3). The stimuli cycled through gray, white, gray, black, and back to gray. The average light level was determined by the intermediate (gray) value of the step sequence, where the gamma corrected display was set to 50% of the maximum output. When the display was set to nominal “black” the output was reduced by 130 fold compared to gray. The photon flux of the “white” step was twice that of the gray.

Receptive field characterization

A stimulus composed of a lattice of squares (pixels), each flickering randomly and independently at 120 Hz (30 Hz in some experiments) was used to characterize the spatiotemporal response properties of recorded RGCs50. The sizes of individual pixels varied from 58 μm to 116 μm on a side. The intensity of each display primary at each pixel location was chosen from a binary distribution at each refresh. At photopic light levels, an RGB white noise stimulus was used: the three display primaries at each pixel location varied independently of one another. The contrast of this stimulus for each of the three display primaries was 96% (difference between the maximum and minimum intensities divided by the sum of intensities). In some experiments at scotopic light levels an RGB white noise stimulus was used. In other experiments a black-and-white (BW) white noise stimulus was presented: the three display primaries were modulated together at each pixel location with a contrast of 96%. The BW white noise stimulus generated a higher effective contrast because the display primaries were modulated synchronously. This allowed receptive fields of equal signal-to-noise ratios to be estimated in less time, but this stimulus does not provide spectral information about the RGC light responses. Control analyses indicated that the BW stimulus did not introduce a bias in receptive field size estimates compared to the RGB stimulus. Typically, STAs were calculated from either 15 or 30 minute presentations of the white noise stimulus.

SBC receptive fields were summarized by fitting with a parametric model. The model consisted of the product of two profiles: spatial and temporal11. The temporal profile was a difference of lowpass filters. The spatial profile consisted of a 2-dimensional elliptical Gaussian function. This model was sufficient to describe the receptive fields measured with BW white noise stimuli under scotopic conditions. For scotopic presentations of RGB white noise, fits included two additional parameters that described the relative sensitivity to contrast modulation of the three display primaries. Photopic stimuli always consisted of

RGB white noise, and only the spatial and temporal profiles of the blue display primary were fit. This fit accurately described the S cone mediated receptive field center of the SBCs11. Several parameters of the fits were extracted to visualize receptive field extent: the location of the Gaussian fit center, the s.d. along the major and minor axes, and the angle of the major axis. These parameters defined an ellipse for each cell that represented the 1 s.d. contour of the Gaussian fit. In the figures, receptive field outlines are represented using this contour.

Cell Type Classification and Identification

The morphological type of recorded cells was determined using a two step procedure, as described previously11. Briefly, cells were first grouped into functional classes based on light response properties. Functional classes were identified by distinct clustering of cells according to response properties (Fig. 1b,**g**). At the high light level (Fig. 1b), two response properties distinguished SBCs from all other ON type RGCs: the ratio of the peak amplitudes of the STA time courses to the green and blue monitor primaries, and the receptive field radius. The receptive field radius was given by the radius of a circle with an area equal to that defined by the 1 s.d. contour of the two dimensional Gaussian fit to the spatial profile of the STA. At the low light level (Fig. 1g), SBCs were functionally classified based on the receptive field radius and the weights associated with the first principal component (PC) of the STA time courses. These weights were obtained by performing principal components analysis on the concatenated STA time courses associated with the red, green and blue display primaries. Correspondences between functional classes and morphological types were determined by cell density and light response properties. This procedure definitively identified the SBCs in each recording 11.

Electrophysiological Image

After the spikes from a given neuron were isolated on a source electrode, the average electrical activity in a time window from 0.5 ms before to 3 ms after the spike was calculated across the electrode array10. Because the spiking activity of any given cell is largely independent from all other cells, the average electrical activity across the array reveals a unique electrical “footprint” for every cell, reflecting its position, width of dendritic arbor, and axon trajectory relative to the electrode array. EIs are displayed as a dot pattern where each dot represents the location of an electrode where the signal from the neuron was detected and the diameter of the dot is proportional to the amplitude of the peak of the signal over time (Fig. 1c–**e**,**h**–**j**).

The uniqueness of the EI for a given cell across an experiment was confirmed by calculating the correlation coefficient between the EI of a reference cell in recording *A* to the EIs of all the cells in recording *B*, e.g. between high and low light levels. Accumulated across all (53) SBCs in three representative preparations, the EI with the highest correlation coefficient in recording *B* was always given by a cell that was a member of the functional class that formed a mosaic with a conserved spatial organization to that observed in recording *A*, and whose receptive field overlapped with the reference cell in *A*. The uniqueness of the EI allowed cells to be tracked from one recording condition to another.

Anatomy

Two *Macaca mulata* and one *Macaca fascicularis* were euthanized with an overdose of pentobarbital, following a protocol approved by the institutional Animal Welfare Committee. The eyes were removed, the anterior half was discarded, and the vitreous humor was removed from the posterior half with fine forceps. For the *M. mulata*, pieces of the eyecup were fixed with 4% paraformaldehyde in 0.1 M sodium phosphate buffer pH 7.4 overnight at 4 C. The retinas were isolated and rinsed with PBS. For the *M. fascicularis*, the retina was fixed for 2 hrs at 20 C with 0.1% glutaraldehyde added to the primary fixative. It was then treated with 1% NaBH in PBS for 60 mins. The retinas were embedded in agarose; then 50–70 μm vertical sections were cut with a VT1000S microtome (LEICA). The sections were incubated for 14 days at 4C in PBS pH 7.4 with 5% Chemiblock (Millipore) and 0.3% Triton X-100 (Sigma) and the following primary antibodies: goat anti-calretinin (1:1000, Chemicon), rabbit anti-G6-gly (1:1000) and mouse monoclonal antibody to connexin 36 (1:1000, Chemicon). The tissue was then incubated for 2 hrs at 20 C in PBS with 5% Chemiblock, 0.3% Triton X-100 and the following affinity-purified secondary antibodies raised in donkeys: Cy3 anti-goat IgG (1:1000, Jackson ImmunoResearch), Alexa 488 anti-rabbit IgG (1:1000, Molecular Probes) and Cy5 anti-mouse IgG (1:500, Jackson ImmunoResearch). The images were acquired using a Zeiss LSM 510 confocal laser scanning microscope; illustrations were prepared using LSM (Zeiss) and Photoshop 6.0 (Adobe) software.

Supplementary Material

Refer to Web version on PubMed Central for supplementary material.

Acknowledgments

This work was supported by the Helen Hay Whitney Foundation (G.D.F.), DFG (M.G.), NIH NRSA (NS054519-01) and Chapman Foundation (J.L.G.), Miller Institute for Basic Research in Science, University of CA, Berkeley (J.S.), Burroughs Wellcome Fund Career Award at Scientific Interface (A.S.), McKnight Foundation (A.M.L. & E.J.C.), NSF Grant PHY-0750525 (A.M.L.), a Sloan Research Fellowship, and NIH Grant EY13150 (E.J.C), EY06472 (D.W.M) and EY10608 (D.W.M). We thank C.K. Hulse for technical assistance; M.I. Grivich, D. Petrusca, W. Dabrowski, A. Grillo, P. Grybos, P. Hottowy, and S. Kachiguine for technical development; H. Fox, M. Taffe, E. Callaway and K. Osborn for providing access to retinas; H. Wassle and J. O'Brien for providing antibodies; S. Barry for machining. We thank the San Diego Supercomputer Center and the NSF (Cooperative Agreements 05253071 and 0438741) for large scale data storage.

References

1. Masland R. The fundamental plan of the retina. Nat Neurosci. 2001; 4:877–886. [PubMed: 11528418]
2. Dacey, D. Origins of perception: retinal ganglion cell diversity and the creation of parallel visual pathways. In: Gazzaniga, M., editor. The Cognitive Neurosciences. MIT Press; 2004. p. 281-301.
3. Field G, Chichilnisky E. Information processing in the primate retina: circuitry and coding. Annu Rev Neurosci. 2007; 30:1–30. [PubMed: 17335403]
4. Dacey D, Lee B. The 'blue-on' opponent pathway in primate retina originates from a distinct bistratified ganglion cell type. Nature. 1994; 367:731–735. [PubMed: 8107868]
5. Szmajda B, Grunert U, Martin P. Retinal ganglion cell inputs to the koniocellular pathway. J Comp Neurol. 2008; 510:251–268. [PubMed: 18626946]
6. Buck, S. Rod-cone interactions in human vision. In: Chalupa, LM.; Werner, JS., editors. Neurosciences, T V. The MIT Press; Cambridge: 2004. p. 863-878.

7. Lee B, Smith V, Pokorny J, Kremers J. Rod inputs to macaque ganglion cells. Vision Res. 1997; 37:2813–2828. [PubMed: 9415362]
8. Wiesel T, Hubel D. Spatial and chromatic interactions in the lateral geniculate body of the rhesus monkey. J Neurophysiol. 1966; 29:1115–1156. [PubMed: 4961644]
9. Virsu V, Lee B. Light adaptation in cells of macaque lateral geniculate nucleus and its relation to human light adaptation. J Neurophysiol. 1983; 50:864–878. [PubMed: 6631467]
10. Litke A, et al. What does the eye tell the brain? development of a system for the large scale recording of retinal output activity. IEEE Trans Nucl Sci. 2004:1434–1440.
11. Field G, et al. Spatial properties and functional organization of small bistratified ganglion cells in primate retina. J Neurosci. 2007; 27:13261–13272. [PubMed: 18045920]
12. Kolb H, Famiglietti E. Rod and cone pathways in the inner plexiform layer of cat retina. Science. 1974; 186:47–49. [PubMed: 4417736]
13. Bloomfield S, Dacheux R. Rod vision: pathways and processing in the mammalian retina. Prog Retin Eye Res. 2001; 20:351–384. [PubMed: 11286897]
14. Chichilnisky E, Baylor D. Receptive-field microstructure of blue-yellow ganglion cells in primate retina. Nature Neurosci. 1999; 2:889–893. [PubMed: 10491609]
15. Rodieck, R. The first steps in seeing. Sinauer; Sunderland, MA: 1998.
16. Sharpe L, Stockman A. Rod pathways: the importance of seeing nothing. Trends Neurosci. 1999; 22:497–504. [PubMed: 10529817]
17. Gouras P, Link K. Rod and cone interaction in dark-adapted monkey ganglion cells. J Physiol. 1966; 184:499–510. [PubMed: 4958644]
18. Cleland B, Levick W. Properties of rarely encountered types of ganglion cells in the cat's retina and an overall classification. J Physiol. 1974; 240:457–492. [PubMed: 4420300]
19. Barlow H, Fitzhugh R, Kuffler S. Change of organization in the receptive fields of the cat's retina during dark adaptation. J Physiol. 1957; 137:338–354. [PubMed: 13463771]
20. Troy J, Bohnsack D, Diller L. Spatial properties of the cat x-cell receptive field as a function of mean light level. Vis Neurosci. 1999; 16:1089–1104. [PubMed: 10614589]
21. Peichl L, Wassle H. The structural correlate of the receptive field centre of alpha ganglion cells in the cat retina. J Physiol. 1983; 341:309–324. [PubMed: 6620182]
22. Field G, Sampath A, Rieke F. Retinal processing near absolute threshold: from behavior to mechanism. Ann Revs Physiol. 2005; 67
23. Hornstein E, Verweij J, Li P, Schnapf J. Gap-junctional coupling and absolute sensitivity of photoreceptors in macaque retina. J Neurosci. 2005; 25:11201–11209. [PubMed: 16319320]
24. Volgyi B, Deans M, Paul D, Bloomfield S. Convergence and segregation of the multiple rod pathways in mammalian retina. J Neurosci. 2004; 24:11182–11192. [PubMed: 15590935]
25. Slaughter M, Miller R. 2-amino-4-phosphonobutyric acid: a new pharmacological tool for retina research. Science. 1981; 211:182–185. [PubMed: 6255566]
26. Muller F, Wassle H, Voigt T. Pharmacological modulation of the rod pathway in the cat retina. J Neurophysiol. 1988; 59:1657–1672. [PubMed: 3404200]
27. Murphy G, Rieke F. Network variability limits stimulus-evoked spike timing precision in retinal ganglion cells. Neuron. 2006; 52:511–524. [PubMed: 17088216]
28. Cohen E, Sterling P. Demonstration of cell types among cone bipolar neurons of cat retina. Philos Trans R Soc Lond B Biol Sci. 1990; 330:305–321. [PubMed: 1982357]
29. Marshak D, Aldrich L, Del Valle J, Yamada T. Localization of immunoreactive cholecystokinin precursor to amacrine cells and bipolar cells of the macaque monkey retina. J Neurosci. 1990; 10:3045–3055. [PubMed: 2398370]
30. Wassle H, Grunert U, Chun M, Boycott B. The rod pathway of the macaque monkey retina: identification of aii-amacrine cells with antibodies against calretinin. J Comp Neurol. 1995; 361:537–551. [PubMed: 8550898]
31. Mills S, O'Brien J, Li W, O'Brien J, Massey S. Rod pathways in the mammalian retina use connexin 36. J Comp Neurol. 2001; 436:336–350. [PubMed: 11438934]

32. Lyubarsky A, Daniele L, Pugh EJ. From candelas to photoisomerizations in the mouse eye by rhodopsin bleaching in situ and the light-rearing dependence of the major components of the mouse erg. Vision Res. 2004; 44:3235–3251. [PubMed: 15535992]
33. Calkins D, Tsukamoto Y, Sterling P. Microcircuitry and mosaic of a blue-yellow ganglion cell in the primate retina. J Neurosci. 1998; 18:3373–3385. [PubMed: 9547245]
34. Veruki M, Hartveit E. Electrical synapses mediate signal transmission in the rod pathway of the mammalian retina. J Neurosci. 2002; 22:10558–10566. [PubMed: 12486148]
35. Petrides A, Trexler E. Differential output of the high-sensitivity rod photoreceptor: Aii amacrine pathway. J Comp Neurol. 2008; 507:1653–1662. [PubMed: 18241050]
36. Jacoby R, Marshak D. Synaptic connections of db3 diffuse bipolar cell axons in macaque retina. J Comp Neurol. 2000; 416:19–29. [PubMed: 10578100]
37. Dunn F, Lankheet M, Rieke F. Light adaptation in cone vision involves switching between receptor and post-receptor sites. Nature. 2007; 449:603–606. [PubMed: 17851533]
38. Grunert U. Anatomical evidence for rod input to the parvocellular pathway in the visual system of the primate. Eur J Neurosci. 1997; 9:617–621. [PubMed: 9104603]
39. Dacey D, et al. Melanopsin-expressing ganglion cells in primate retina signal colour and irradiance and project to the lgn. Nature. 2005; 433:749–754. [PubMed: 15716953]
40. Dacey D, Packer O. Colour coding in the primate retina: diverse cell types and cone-specific circuitry. Curr Opin Neurobiol. 2003; 13:421–427. [PubMed: 12965288]
41. Schein S, Sterling P, Ngo I, Huang T, Herr S. Evidence that each s cone in macaque fovea drives one narrow-field and several wide-field blue-yellow ganglion cells. J Neurosci. 2004; 24:8366–8378. [PubMed: 15385619]
42. von Kries J, Nagel W. Uber den Einfluss von Lichtstarke und Adaptation auf das Sehen des Dichromaten (Grunblinden). Zeitschrift fur Psychologie und Physiologie der Sinnesorgane. 1896; 12:1–36.
43. Knight R, Buck S, Fowler G, Nguyen A. Rods affect s-cone discrimination on the farnsworth-munsell 100-hue test. Vision Res. 1998; 38:3477–3481. [PubMed: 9893868]
44. Cao D, Zele A, Pokorny J. Chromatic discrimination in the presence of incremental and decremental rod pedestals. Vis Neurosci. 2008; 25:399–404. [PubMed: 18598409]
45. Buck S, Knight R, Bechtold J. Opponent-color models and the influence of rod signals on the loci of unique hues. Vision Res. 2000; 40:3333–3344. [PubMed: 11058732]
46. Cao D, Pokorny J, Smith V, Zele A. Rod contributions to color perception: linear with rod contrast. Vision Res. 2008; 48:2586–2592. [PubMed: 18561973]
47. Baylor D, Nunn B, Schnapf J. The photocurrent, noise and spectral sensitivity of rods of the monkey macaca fascicularis. J Physiol. 1984; 357:575–607. [PubMed: 6512705]
48. Baylor D, Nunn B, Schnapf J. Spectral sensitivity of cones of the monkey macaca fascicularis. J Physiol. 1987; 390:145–160. [PubMed: 3443931]
49. Schnapf J, Nunn B, Meister M, Baylor D. Visual transduction in cones of the monkey macaca fascicularis. J Physiol (Lond). 1990; 427:681–713. [PubMed: 2100987]
50. Chichilnisky E. A simple white noise analysis of neuronal light responses. Network: Computation in Neural Systems. 2001; 12:199–213.

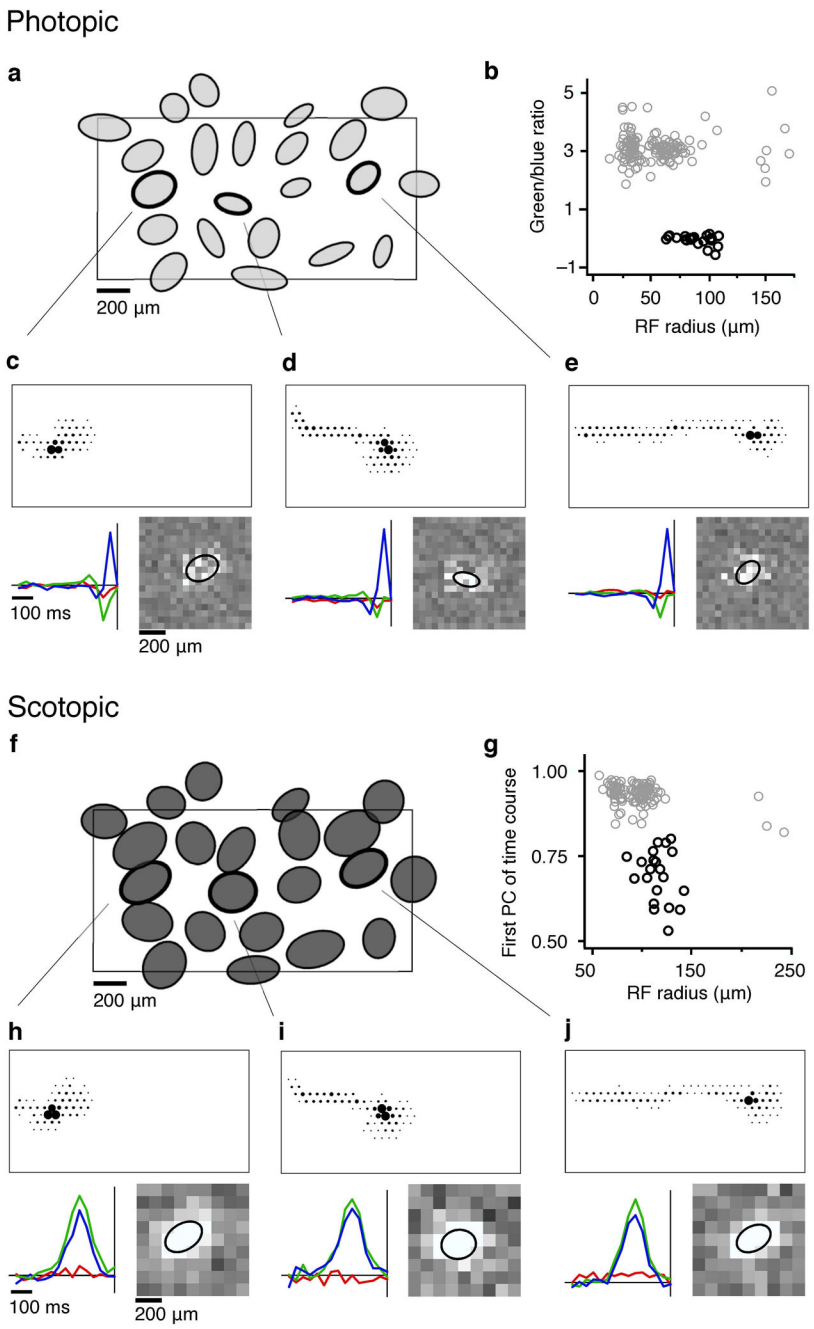

Figure 1.

SBC identification at photopic and scotopic light levels (**a**) Spatial receptive fields of 22 simultaneously recorded SBCs at <800 (see Methods) P*/cone/s. Ellipses represent the 1 s.d. contour of a fit to the blue-ON receptive field (see Methods). Rectangle indicates the outline of the electrode array (1800 × 900 μm). (**b**) Scatter plot shows the classification of SBCs (black circles) that distinguishes them from all other ON RGCs (gray circles, see Methods) (**c**–**e**), Three cells are highlighted from the receptive field mosaic in **a**. Top: the electrophysiological image (EI; see Methods). Lower left: STA time course for each display

primary: red, green and blue. The abscissa indicates the time to the spike, the ordinate indicates the primary intensities relative to background (arbitrary units: a.u.). Bottom right: spatial profile of the STAs from the blue primary; ellipse is 1 s.d. contour from fit. (**f**) Spatial receptive fields of the cells in **a** estimated at 1.2 P*/rod/s. (**g**) Scatter plot shows the classification of SBCs at the low light level (black circles, see Methods). (**h–j**) The EIs (top) and STA time courses and spatial profiles (bottom) measured at the low light level for the same cells as **c–e**. Spatial profiles are from the sum of the blue and green primaries.

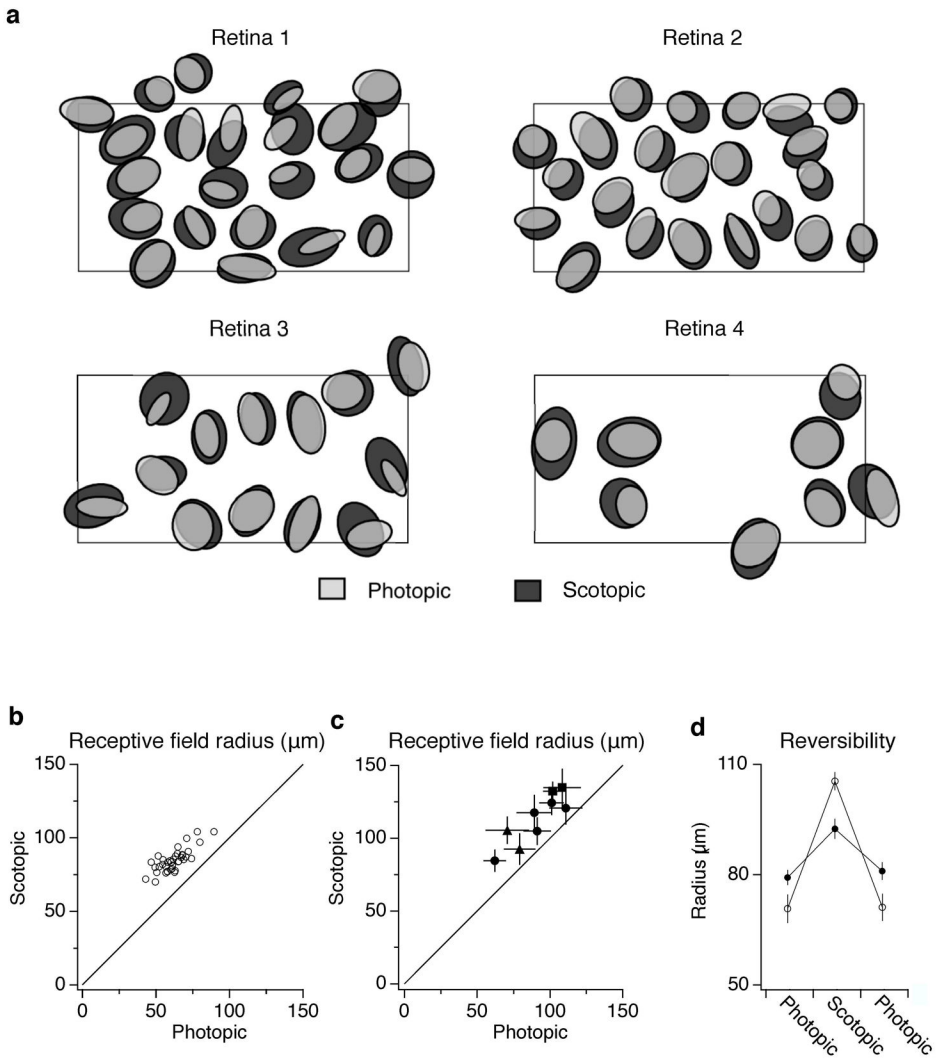

Figure 2.

Change in SBC receptive field size between scotopic and photopic light levels. (**a**) Overlaid rod mediated (dark gray) and S cone mediated (light gray) receptive fields from four recordings. Retina 1 is the same as that in Fig. 1. The rod mediated receptive fields for retinas 1–3 were measured at 1.2 P*/rod/s, and those for retina 4 were measured at 0.077 P*/rod/s. Rectangles indicate the outline of the electrode array. (**b**) Comparison of receptive field size (radius of circle with area equal to ellipse) between rod and cone dominated conditions in a single preparation. (**c**) Comparison of receptive field radius across 8 preparations. Circles and squares display preparations where the scotopic light level was 1.2 and 0.077 Rh*/rod/s respectively. Triangles represent preparations in which the pigment epithelium remained attached to the retina (see Methods) and the scotopic light level was 1.5 P*/rod/s. Error bars are 1 s.d. (**d**) Receptive field size was averaged across 17 (filled circles) and 15 (open circles) SBCs in two preparations with the pigment epithelium attached to the retina. The light level was transitioned from cone (<1000 P*/cone/s), to rod (1.5 P*/rod/s), and back to cone light levels. Error bars are ±1 s.e.m.

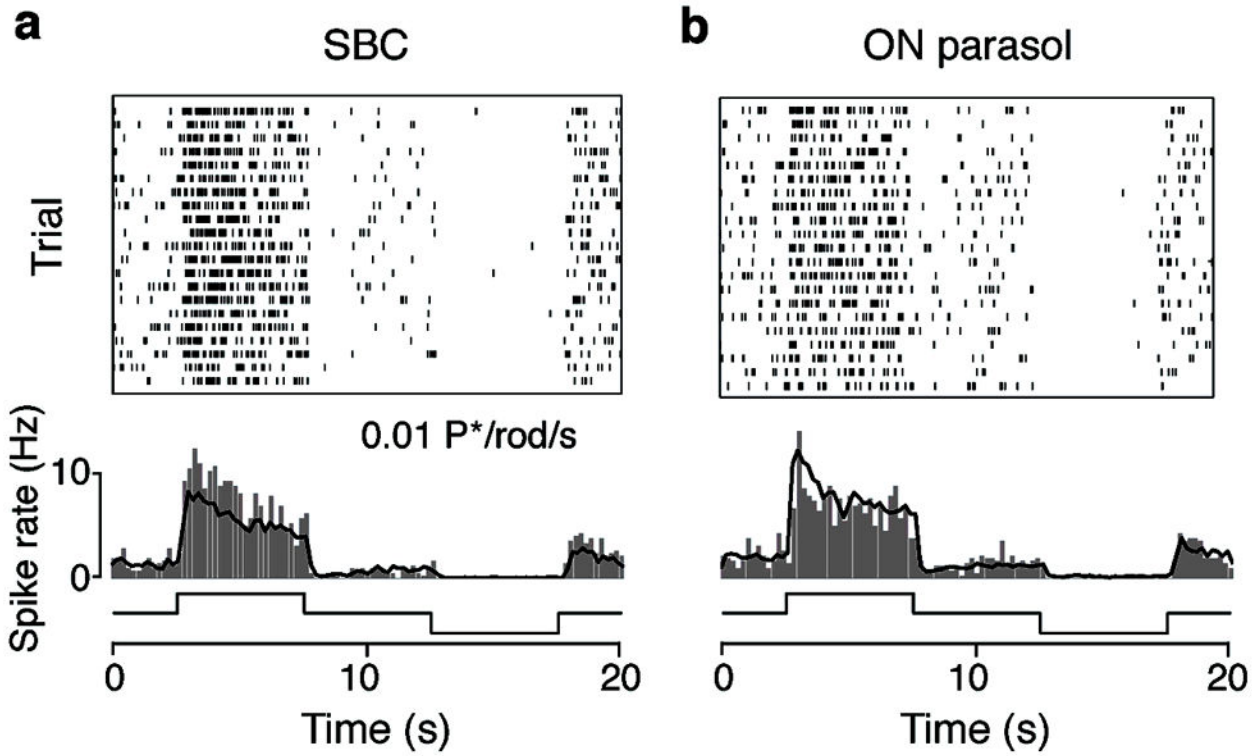

Figure 3.

Responses of SBCs and ON parasol cells to dim light steps. (**a**) Top: spike rasters from a single SBC in response to 20 repetitions of full field light steps that transitioned every 5 s from gray (0.01 P*/rod/s), to white (0.02 P*/rod/s), to gray, to nominal black (0.00008 P*/rod/s). Middle: peri-stimulus time histrogram (PSTH; bin size = 0.2 s) of the response of an individual SBC (gray bars) and the average from 6 simultaneously recorded SBCs (black trace). Bottom: time course of the stimulus. (**b**) Top: spike raster from a single ON parasol cell recorded simultaneously with the SBC in **a**. Middle: PSTH of the ON parasol cell (gray bars) and average from 23 ON parasol cells recorded simultaneously. Bottom: time course of stimulus.

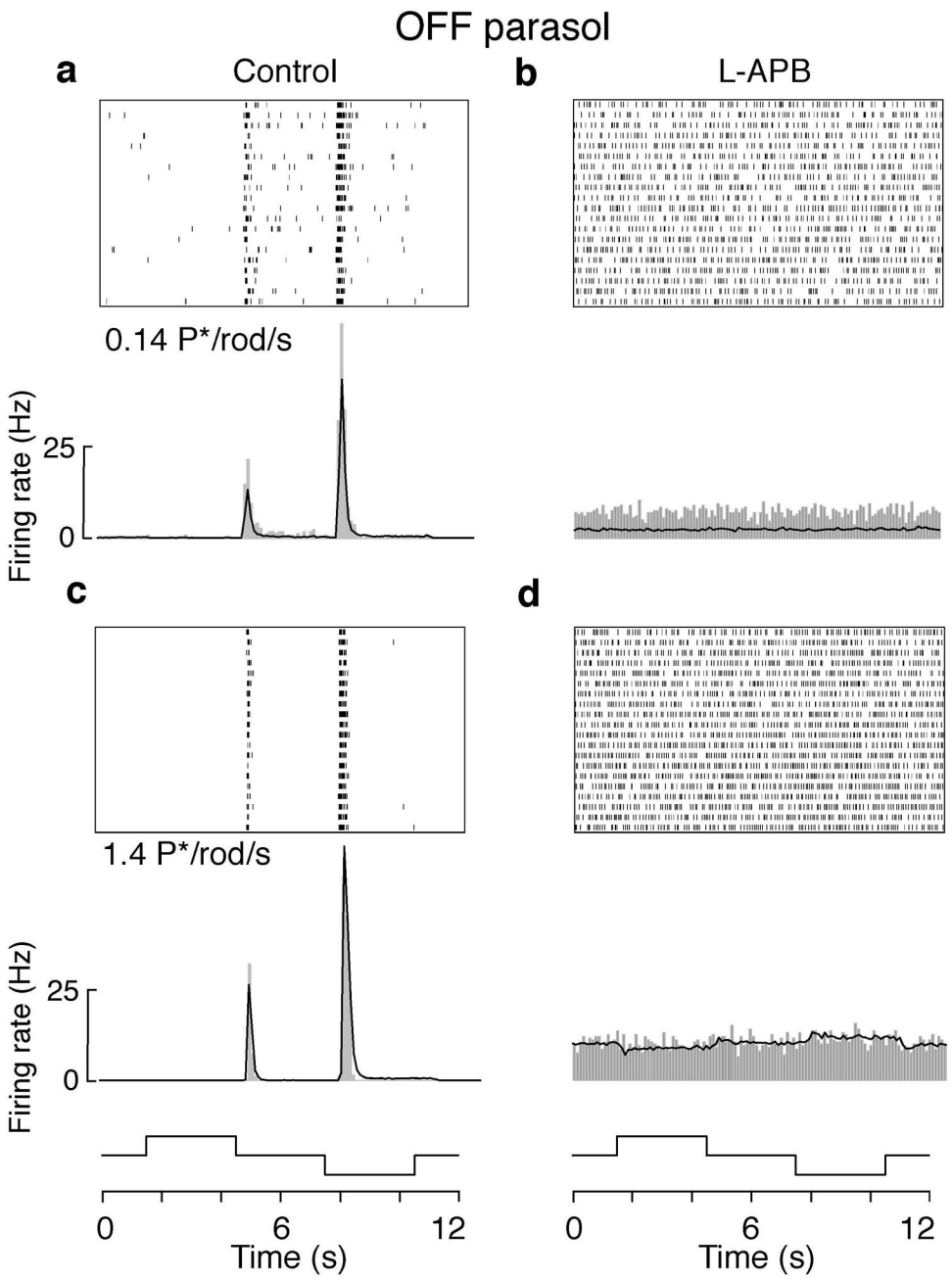

Figure 4.

L-APB nearly eliminated the light response in OFF parasol cells at low scotopic conditions. (**a**) Top: spike rasters from a single OFF parasol cell in response to 20 repetitions of full field light steps that transitioned every 3 s from gray (0.14 P*/rod/s), to white (0.28 P*/rod/s), to gray, to nominal black (0.0005 P*/rod/s). Bottom: PSTH (bin size = 0.1 s) of the OFF parasol cell (gray bars) and the average from 24 simultaneously recorded OFF parasol cells (black trace). (**b**) Same individual cell and population of cells as in **a**, with bath application of 10μM L-APB. (**c**) Same individual and population of cells as in **a**, stimulated

at light levels 10 fold higher: gray = 1.4 P*/rod/s, white = 2.8 P*/rod/s, black = 0.005 P*/rod/s. (**d**) Same as **c** with 10 μM L-APB.

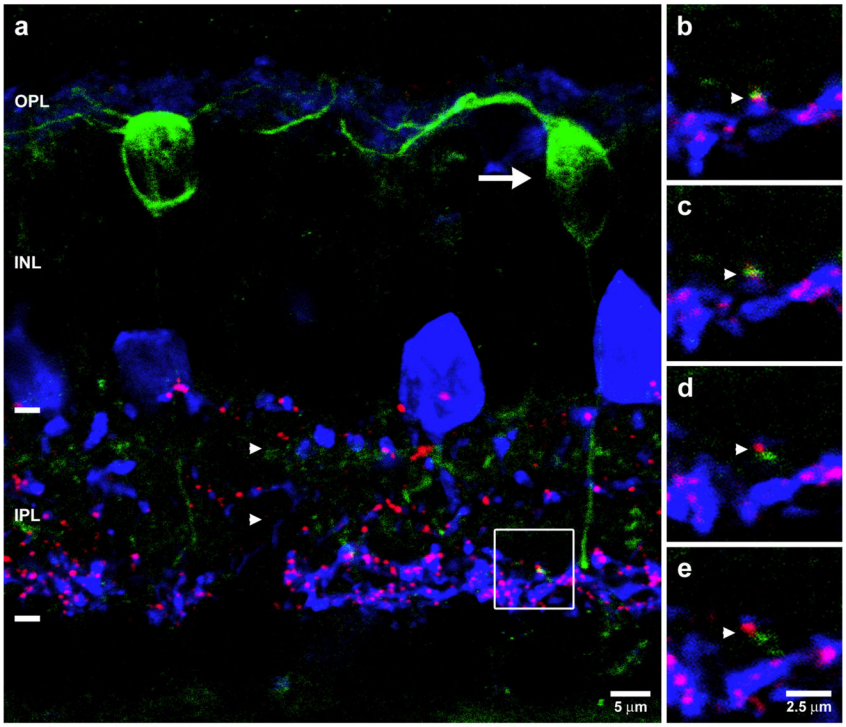

Figure 5.

Gap junctions are present at appositions between AII amacrine and S cone bipolar cells. (**a**) A stack of 5 optical sections of triple labeled macaque retina containing: 2 S cone bipolar cells labeled with anti-G6-gly (green), 4 AII amacrine cells labeled with anti-calretinin (blue) and numerous connexin 36-immunoreactive puncta (red). The large arrow indicates the perikaryon of the S cone bipolar cell. Note the characteristic, laterally oriented dendrites in the outer plexiform layer and the axon descending to S5 of the IPL. The small arrowheads indicate the strata containing labeled amacrine cell dendrites. One of the labeled S cone bipolar cell axon terminals contacts an AII amacrine cell dendrite, and a labeled punctum is present at the site (square). (**b–e**) Consecutive single optical sections of the region indicated by the square in **a** are shown at higher magnification. Arrowheads in **b–e** identify the contact location. OPL: outer plexiform layer; INL: inner nuclear layer; IPL: inner plexiform layer.

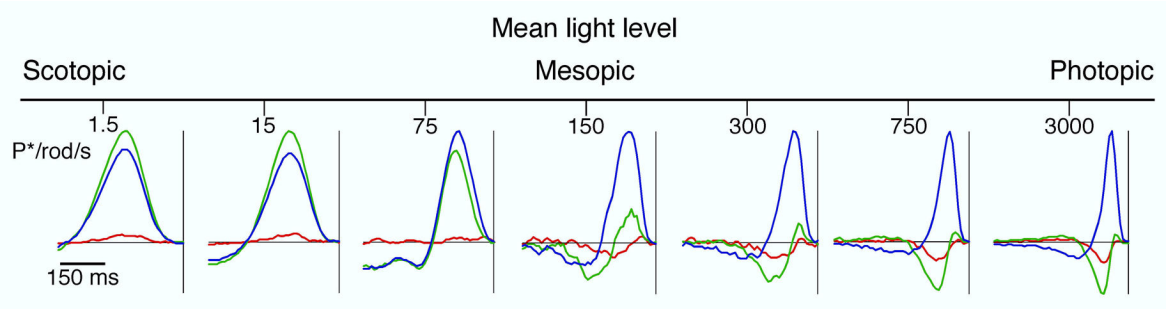

Figure 6.

Spectral tuning of SBC responses depended on light level. In a single recording containing 33 SBCs, the mean STA time courses of the SBCs for the red, green and blue display primaries are shown at seven light levels. The light level increases from left to right. At 3000 P*/rod/s, the rods were saturated, and the response was mediated by the cones. Photoisomerization rates for the L, M and S cones were 1400, 1200, and 430 P*/cone/s, respectively. The SBCs displayed color opponency; increments in the blue display primary and decrements in the red and green display primaries tended to precede spikes. At 150 P*/rod/s, the spectral tuning of the SBCs exhibited a marked change; the SBCs continued to display color opponent responses, but increments rather than decrements in the green display primary tended to precede spikes. At 1.5 P*/rod/s, the light level was below cone threshold, and the spectral tuning of the response was non-opponent reflecting pure rod input to the SBCs.